



This is a repository copy of *Analysis of flux barrier effect of LCF PM in series hybrid magnet variable flux memory machine*.

White Rose Research Online URL for this paper:

<https://eprints.whiterose.ac.uk/207600/>

Version: Published Version

Article:

Huang, Y. orcid.org/0000-0002-0190-4234, Yang, H. orcid.org/0000-0002-2867-5574, Zheng, H. et al. (2 more authors) (2023) Analysis of flux barrier effect of LCF PM in series hybrid magnet variable flux memory machine. *AIP Advances*, 13 (2). 025230. ISSN 2158-3226

<https://doi.org/10.1063/9.0000611>

Reuse

This article is distributed under the terms of the Creative Commons Attribution (CC BY) licence. This licence allows you to distribute, remix, tweak, and build upon the work, even commercially, as long as you credit the authors for the original work. More information and the full terms of the licence here:

<https://creativecommons.org/licenses/>

Takedown

If you consider content in White Rose Research Online to be in breach of UK law, please notify us by emailing eprints@whiterose.ac.uk including the URL of the record and the reason for the withdrawal request.







eprints@whiterose.ac.uk
<https://eprints.whiterose.ac.uk/>

RESEARCH ARTICLE | FEBRUARY 06 2023

Analysis of flux barrier effect of LCF PM in series hybrid magnet variable flux memory machine

Special Collection: [67th Annual Conference on Magnetism and Magnetic Materials](#)

Yunrui Huang ; Hui Yang  ; Hao Zheng; Heyun Lin ; Z. Q. Zhu

 Check for updates

AIP Advances 13, 025230 (2023)
<https://doi.org/10.1063/9.0000611>


View
Online


Export
Citation

 CrossMark



APL Energy
Latest Articles Online!

Read Now

 AIP
Publishing

Analysis of flux barrier effect of LCF PM in series hybrid magnet variable flux memory machine

Cite as: AIP Advances 13, 025230 (2023); doi: 10.1063/9.0000611

Submitted: 4 October 2022 • Accepted: 13 December 2022 •

Published Online: 6 February 2023



View Online



Export Citation



CrossMark

Yunrui Huang,¹  Hui Yang,^{2,a)}  Hao Zheng,¹ Heyun Lin,¹  and Z. Q. Zhu³

AFFILIATIONS

¹School of Electrical Engineering, Southeast University, Sipailou 2, 210096 Nanjing, China

²Suzhou Research Institute, Southeast University, Linqun Street 339, 215000 Suzhou, China

³Department of Electronic and Electrical Engineering, The University of Sheffield, S1 3JD Sheffield, United Kingdom

Note: This paper was presented at the 67th Annual Conference on Magnetism and Magnetic Materials.

^{a)}Author to whom correspondence should be addressed: huiyang@seu.edu.cn

ABSTRACT

Variable flux memory machines (VFMMs) with series hybrid magnets using both low coercive force (LCF) and high coercive force (HCF) permanent magnets (PMs) have been recognized as a viable candidate for wide-speed-range industrial applications due to the advantages of high torque density and wide speed range. Nevertheless, the adverse effects of LCF PM on the HCF PM in series-type VFMM under different magnetization states (MSs) are still unreported. In this paper, the flux barrier effect (FBE) of the LCF PM existing in series hybrid magnet VFMM is first revealed, and its causes are discussed as well as analyzed in depth on the basis of the equivalent magnetic circuit method and finite-element (FE) analyses. A topology of VFMM with dual-layer PMs is further developed to alleviate the FBE induced from LCF PMs. It can be found that the FBE can be effectively suppressed by employing the dual-layer (DL) PM arrangement and additional leakage flux paths. A prototype of the proposed design is built, and the theoretical and FE results are experimentally verified.

© 2023 Author(s). All article content, except where otherwise noted, is licensed under a Creative Commons Attribution (CC BY) license (<http://creativecommons.org/licenses/by/4.0/>). <https://doi.org/10.1063/9.0000611>

I. INTRODUCTION

Permanent magnets synchronous machines (PMSMs) have been of growing research interest and extensively investigated.¹⁻³ The utilization of high coercive force (HCF) PMs with high magnetic energy product enables conventional PMSMs to achieve high torque density and high efficiency. However, when the PMSMs work in high speed region, the strong magnetic flux generated by HCF PMs also result in high voltage, causing limited speed range. The negative d -axis flux-weakening control is employed to counteract the induced voltage and expand the speed range.^{4,5} However, the continuous d -axis flux-weakening current leads to additional excitation copper loss, which makes the conventional PMSMs still suffers from the compromised efficiency in high-speed region.

Variable flux memory machines (VFMMs) equipped with LCF PMs have been proposed to solve the problem.⁶⁻¹⁴ The magnetization state (MS) of low coercive force (LCF) PM can be magnetized or demagnetized by a current pulse with negligible excitation copper loss, so that the flux linkage of this type of machine can be varied

appropriately to improve the efficiency in the flux-weakening region. Those single LCF PM based VFMMs can easily achieve online flux regulation, albeit with sacrificed torque density. Meanwhile, the machine reliability is compromised because the unintentional demagnetization may occur under high load current, especially when the negative d -axis current is employed to obtain reluctance torque.

Normally, the hybrid magnet VFMM topologies having both HCF and LCF PMs are applied to achieve improved torque density and extended constant power speed range simultaneously. In, the LCF PMs and HCF PMs are connected in parallel in the magnetic circuit. However, due to the cross-coupling effect between two kinds of PMs, unintentional demagnetization problem is still unsolved, reducing the torque density of parallel-type VFMM. Considering the fact that LCF PM is vulnerable to the load current, series hybrid magnet VFMM is proposed, in which two kinds of PMs are magnetically connected in series so that the HCF PM flux can elevate the working point of the LCF PMs. This can stabilize the on-load MS of LCF PM and the torque density is accordingly improved.¹¹ Nevertheless, the

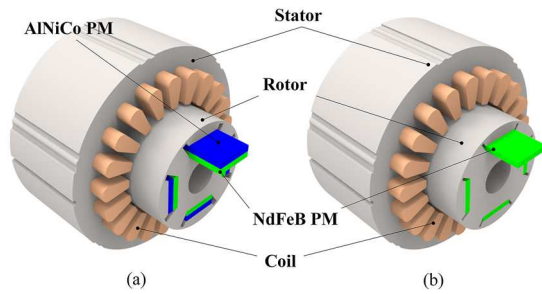


FIG. 1. Machine topologies. (a) Conventional series hybrid magnet VFMM. (b) Benchmark machine.

unique role LCF PM acts in the series magnetic circuit and its potential effect on the HCF magnet as well as air-gap flux density remains unclear. The cross-coupling effect still exists between the two kinds of PMs, and it is quite complicated since the effect varies significantly with the MS of the LCF PM.

In this paper, the FBE of LCF PM in a series hybrid magnet VFMM is first revealed and investigated using a conventional single HCF PM based machine as a reference by removing the LCF PMs. It is proved the FBE can weaken the air-gap flux density based on the magnetic circuit analysis and FE analyses, which further leads to the torque density reduction. In order to address this issue, an approach to preventing the air-gap flux density drop is presented by arranging PM in a dual-layer (DL) pattern.¹⁴ The DL PM design can restrain the weakening effect of the back EMF caused by the FBE in the flux-enhanced state. Eventually, a prototype machine is manufactured and experimental validation is carried out.

II. FLUX BARRIER EFFECT OF LCF PM IN CONVENTIONAL SERIES VFMM

The topologies of a conventional series hybrid magnet VFMM and a benchmark IPM machine are shown in Figs. 1(a) and 1(b) respectively. The stator structure of the two machine is basically the same, and a 21-stator-slot and 4-rotor-pole combination is commonly employed for both machines. It should be also noted that the benchmark IPM machine can be obtained by removing the LCF magnets in the comparative series-type VFMM. In the conventional series VFMM, the additional LCF AlNiCo PMs are closely attached to the side of the HCF NdFeB PMs adjacent to the air-gap. Two types of PMs are completely physically connected in series in the magnetic circuit, and almost all the HCF PM flux will pass through the LCF PM inevitably. It is worth further mentioning that the width and thickness of HCF PMs used in both machines are identical in order to better reflect the potential FBE of the LCF PM.

In Fig. 2, the equivalent magnetic circuits of both machines are given, in which the magnetic flux leakage and core magnetic reluctance are ignored. In the conventional series hybrid magnet VFMM, the MMF and magnetic reluctance of two different PMs should be analyzed separately. The relationship of magnetic reluctance, MMF and flux can be given by:

$$\phi_1 = \frac{F_{hm} + F_{lm}}{R_{hm} + R_{lm} + R_g} \quad (1)$$

$$\phi_2 = \frac{F_{hm}}{R_{hm} + R_g} \quad (2)$$

$$R_m = \frac{h_m}{\mu_0 \mu_r w_m l} \quad (3)$$

$$F_m = h_m H_c \quad (4)$$

where R and F are the equivalent magnetic reluctance and MMF, respectively. The subscripts hm and lm represent the HCF PMs and LCF PMs, respectively. R_g represents the magnetic reluctance of air-gap. Consequently, the MMF and magnetic reluctance of PM can be calculated by (3) and (4). h_m and w_m are the thickness and width of each PM, respectively. l is the axial length of the rotor. μ_0 is the vacuum permeability and μ_r is the relative permeability of the PM material. H_c is the coercivity of PM. It should be noted that the parameters of HCF PMs and air-gap length in two machines are the same, and thus, the magnetic reluctance and MMF of these parts are also identical. In order to better reflect the adverse FBE which may cause, the FBE coefficient k_f is defined as follows:

$$k_f = \left(\frac{\phi_2 - \phi_1}{\phi_2} \right) \times 100\% = \left(1 - \frac{F_{hm} + F_{lm}}{F_{hm}} \cdot \frac{R_{hm} + R_g}{R_{hm} + R_{lm} + R_g} \right) \times 100\% \quad (5)$$

This coefficient can be used to determine whether the FBE occurs and reduces the air-gap flux density of machine. It should be noted that the ratio of coercivity to magnetic reluctance of AlNiCo PM is significantly lower than that of NdFeB PM. The relative permeability of NdFeB PM is about 1 while the relative permeability of AlNiCo PM is about 1.5, and the coercivity of NdFeB PM is three times higher than that of AlNiCo PM. The air-gap length is much lower than the thickness of HCF PM, and hence R_g is estimated to be 0.1 times the R_h . As a result, the value of k_f can be estimated as follows:

$$k_f \approx 1 - \left(1 + \frac{h_l}{3h_h} \right) \cdot \frac{1.1}{1.1 + \frac{h_l}{1.5h_h}} = 1 - \frac{1.1 + \frac{h_l}{4.5h_h}}{1.1 + \frac{h_l}{1.5h_h}} > 0 \quad (6)$$

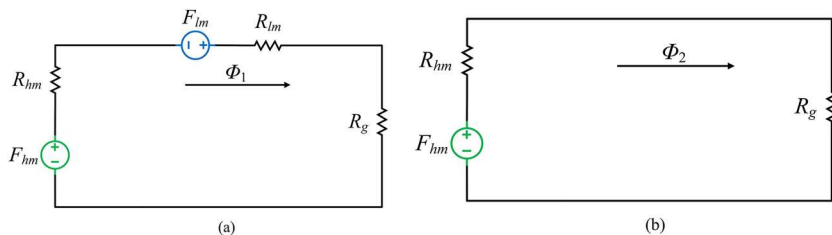


FIG. 2. Equivalent magnetic circuit. (a) Conventional series hybrid magnet VFMM. (b) Benchmark machine.

According to (6), k_f is always positive, and thus the air-gap flux density of conventional series VFMM is also lower than that of the benchmark IPM machine. Therefore, it proves the FBE also exists in the conventional series VFMM. Moreover, the thicker the LCF PM, the more pronounced its effect is. This phenomenon can be explained by the fact that the air-gap flux enhancement by the MMF of the LCF PMs cannot compensate for the weakening effect of the air-gap flux due to the magnetic reluctance of LCF PMs. Furthermore, the FBE will lead to the torque density reduction. Although the LCF PM is added in the series VFMM compared to the benchmark IPM machine, the MMF and magnetic reluctance of LCF PM are responsible for the magnetic flux drop, which indicates that the LCF PM in magnetic circuit can be regarded as a magnetoresistance.

Figure 3 shows the open-circuit back-EMF waveforms of the two machines. It can be observed that the back-EMF amplitude of the VFMM is lower than that of the benchmark machine even the LCF PMs are completely forward magnetized. As a result, the FBE of the LCF PM is confirmed. The flux regulation capability of the conventional series VFMM is limited, because the series connection of the two kinds of PMs makes the LCF PMs always maintained at a high MS by the HCF PM.

In order to further verify the correctness of the foregoing theoretical analysis of the FBE, the back EMF amplitudes of conventional series hybrid magnet VFMMs versus different LCF PM thickness are shown in Fig. 4(a). The variations of FBE coefficients with different LCF PM thickness when machine work in flux-enhanced state are shown in Fig. 4(b). It can be observed that the amplitude of fundamental back-EMF decreases as the thickness of the LCF PM increases, which is consistent with the previous magnetic circuit analyses. It is also shown that as the LCF PM has a large proportion of the excitation source, the FBE of LCF PM is increased, and

the corresponding magnetic flux is greatly weakened. When the thickness of the LCF PM increases, the back-EMF amplitude in flux-weakened state drops more significantly in Fig. 4(a), which means that the flux variation range is increased in this case. The magnetic flux weakening caused by FBE also results in a lower torque density when the VFMM operates in the flux-enhanced state. It can be overall concluded that although the conventional series hybrid magnet VFMM can protect the LCF PM from unintentional demagnetization, it still suffers from the conflict between flux variation ability and torque density caused by the FBE.

III. REDUCTION OF FLUX BARRIER EFFECT WITH DUAL-LAYER PM TOPOLOGY

Based on the foregoing analyses, the close contact of the two types of PMs causes serious cross-coupling effect in conventional series hybrid magnet VFMM, which is mainly responsible for the FBE phenomenon. In order to alleviate the FBE, a DL PM arrangement is applied.¹⁴ The topology of VFMM with DL PMs is shown in Fig. 5(a). Two pieces of tangentially magnetized NdFeB PM are arranged near q -axis and the radially magnetized AlNiCo PM is arranged on the d -axis close to the air-gap side. A bypass leakage flux path is designed along the iron bridge on the rotor surface. Two types of PM form a DL structure and are magnetically connected in series. It should be further noted that, the usages of two kinds of PMs are identical to that of conventional series hybrid magnet VFMM in order to perform a fair comparison.

The separation of the hybrid PMs and the bypass flux path allows the part of HCF PM magnetic flux to enter the air-gap without passing through the LCF PM. In the equivalent magnetic circuit, a new magnetic reluctance R_b , which represents the magnetic reluc-

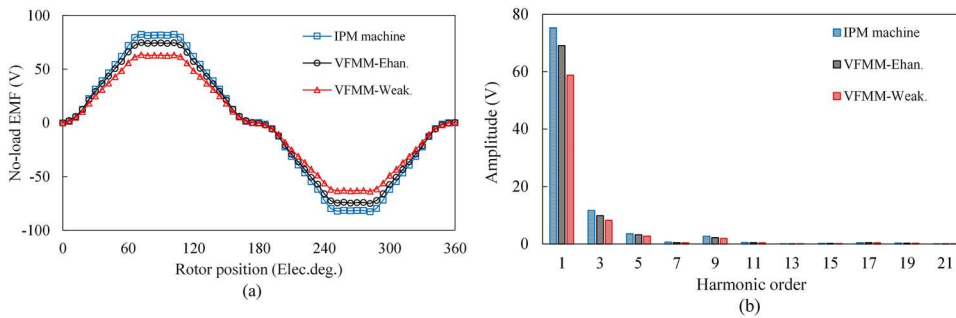


FIG. 3. Back EMF. (a) Waveforms. (b) Spectra.

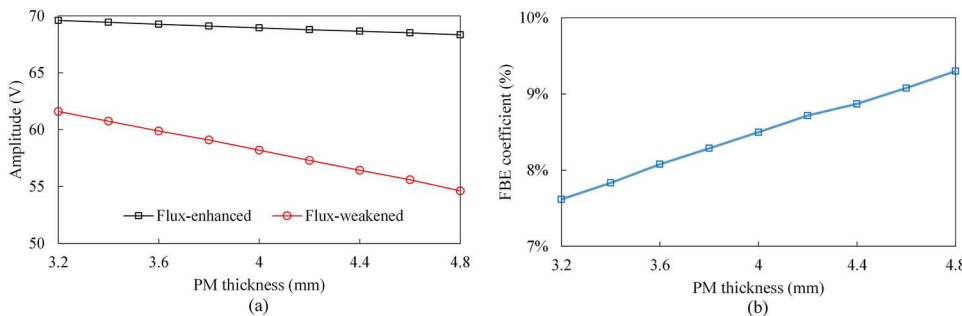


FIG. 4. Effect of PM thickness. (a) Amplitude of fundamental phase back-EMFs versus thickness of the LCF PM. (b) FBE coefficient versus thickness of the LCF PM.

19 January 2024 15:58:45

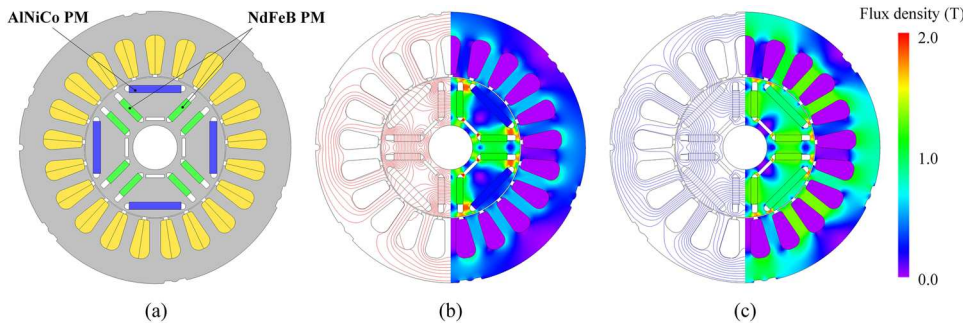


FIG. 5. Open-circuit field and flux line distributions of DL hybrid magnet VFMM. (a) Machine topology. (b) Flux-weakened state (c) Flux-enhanced state.

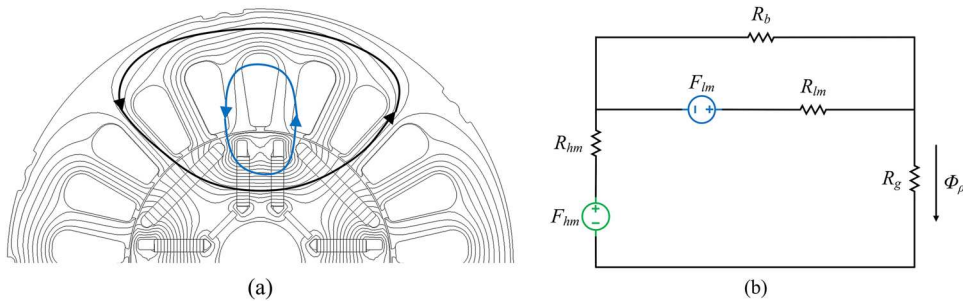


FIG. 6. Field in dual-layer hybrid magnet VFMM. (a) Magnetic flux path schematic. (b) Equivalent magnetic circuit.

tance of bypass flux path is introduced, connects in parallel with the LCF PM. Meanwhile, the DL PM structure makes LCF PM less affected by the HCF PM, which allows the LCF PM to be more easily demagnetized, extending the flux variation range. The corresponding flux distributions of the DL PM VFMM in the flux enhanced and flux weakened states are shown in Figs. 5(b) and 5(c), respectively. When the machine works in the flux enhanced state, the magnetic flux produced by HCF PM mainly pass through the LCF PM. When it turns to flux weakened state, the magnetic flux of HCF PM tends to pass through the bypass flux path instead of LCF PM. This is quite different from the situation of the conventional series VFMM.

Figures 6(a) and 6(b) show the two possible paths of the HCF PM flux into the stator and the equivalent magnetic circuit of dual-layer hybrid magnet VFMM. In the DL hybrid magnet VFMM, the relationship of magnetic reluctance, MMF and flux can be given by:

$$\phi_3 = \frac{F_{hm}}{R_{hm} + R_{lm} // R_b + R_g} + \frac{F_{lm}}{(R_{hm} + R_g) // R_b + R_{lm}} \cdot \frac{R_b}{(R_{hm} + R_g) // R_b} > \frac{F_{hm} + F_{lm}}{R_{hm} + R_{lm} + R_g} \quad (7)$$

$$\phi_3 > \phi_1 \quad (8)$$

In this case, the FBE coefficient k_f can be estimated by:

$$k_f = \left(\frac{\phi_2 - \phi_3}{\phi_2} \right) \times 100\% = \left(1 - \phi_3 \cdot \frac{R_{hm} + R_g}{F_{hm}} \right) \times 100\% \quad (9)$$

It can be seen from the previous analyses that the LCF PM can be equivalent to a magnetoresistance in conventional series VFMM. On the other hand, in DL hybrid magnet VFMM, the equivalent magnetic reluctance of LCF PM is connected in parallel with R_b , which reduces the total reluctance in the magnetic circuit. Consequently, it can be analytically inferred from (7) and (8) that the air-gap flux in DL hybrid magnet VFMM is higher than that in conventional VFMM when the PM parameters are similar.

The variations of FBE coefficients under different LCF magnets MS are given in Fig. 7. The FBE coefficient of conventional series hybrid magnet VFMM is higher than that of DL hybrid magnet VFMM when the LCF MS is the same, which is consistent with the previous analyses. It is worth mentioning that when the LCF PM is

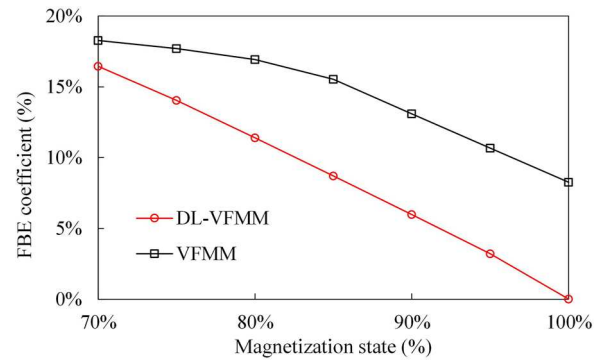


FIG. 7. FBE coefficient versus MS of the LCF PM.

completely forward magnetized, the FBE coefficient of DL VFMM is almost zero, which means the FBE does not occur in the case. The MS change of LCF PM means the MMF of LCF PM varies, but the magnetic permeability of LCF PM hardly changes with its MS. When the MS is low, that is F_l is low, the LCF PM performs like flux barrier and the magnetic reluctance of LCF PM weakens the air-gap flux. When the MS is high, the LCF PM plays a similar role to HCF PM in enhancing magnetic flux density, and the HCF flux still protects the LCF PM from unintentional demagnetization as in conventional series VFMM. The value of the equivalent magnetoresistance decreases as the MS of the LCF PM increases, and even becomes negative under a high LCF MS while in the conventional series hybrid magnet VFMM the value is always positive and varies insignificantly. Therefore, it is confirmed that the FBE of LCF PM is alleviated due to the co-existence of the DL PMs and the bypass flux path.

Figure 8 shows the waveforms of back EMF under different LCF PM MS and the waveforms of torque when the LCF PMs are fully forward magnetized. It can be observed in Fig. 8(a) that the air-gap flux density is increased compared to the conventional series hybrid magnet VFMM and the flux variable range is significantly improved. Meanwhile, the dual-layer PM topology provides higher average torque in Fig. 8(b), which indicates the fact that the FBE of LCF PM in DL VFMM is effectively weakened. Finally, it can be concluded that the FBE of LCF PM can be effectively suppressed with

the DL PM design under different MSs, which is beneficial to the improvement of torque density.

IV. EXPERIMENTAL VERIFICATION

In order to validate the previous analyses on the DL hybrid magnet VFMM, a prototype machine is fabricated. Fig. 9(a) shows the rotor laminations and the prototype machine. The FE predicted and measured open-circuit back-EMF waveforms of the DL series hybrid magnet VFMM prototype under different MSs when the machine runs at 1500 rpm are shown in Fig. 9(b). It can be seen that the measured and simulated results of the prototype under two MSs are basically consistent.

Considering the fact that flux linkage cannot be measured directly, the open-circuit back-EMF amplitude after the current pulse is applied is measured to reflect the flux regulation characteristics. Thus, Fig. 10 compares the FE predicted and measured machine demagnetization and magnetization characteristics. Overall, the measured results agree well with the FE predictions, which indicate that the MS of LCF PM can be adjusted by the current pulse, but the measured magnetization characteristics are slightly different from the simulation because of the difference between the simulation B-H model of LCF PM and the actual one. Fig. 11 compares the FE predicted and measured electromagnetic torque versus different current angle under different MSs. The measured

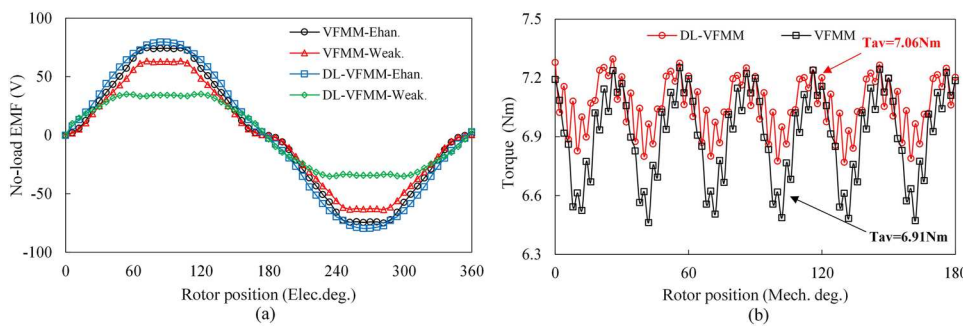


FIG. 8. Performance of dual-layer hybrid magnet VFMM. (a) Waveforms of back EMF. (b) Steady-state torque waveform under flux enhanced state.

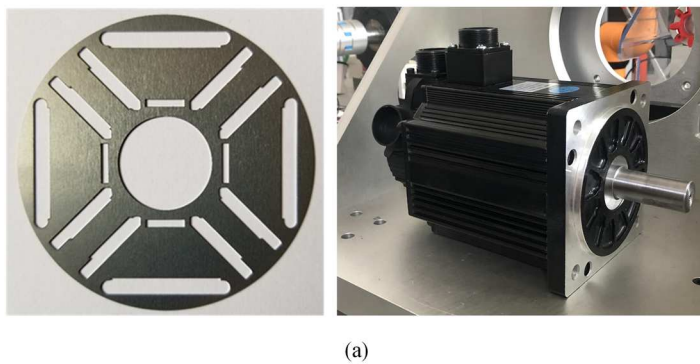


FIG. 9. Test results of back-EMF. (a) Prototype. (b) Back-EMFs (1500 rpm).

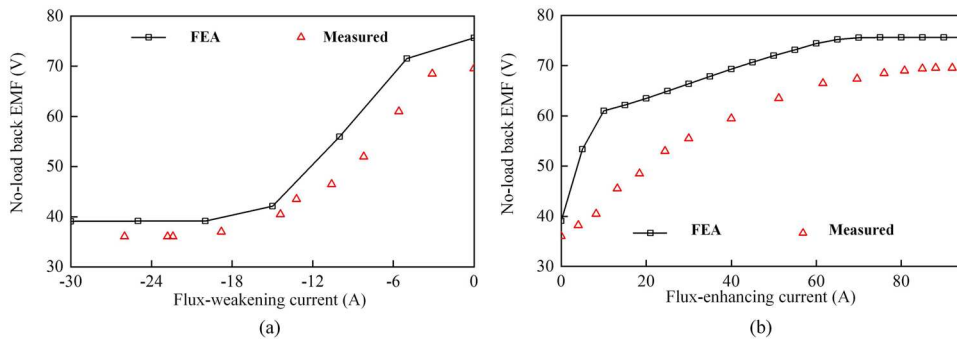


FIG. 10. (a) Demagnetization characteristics. (b) Magnetization characteristics.

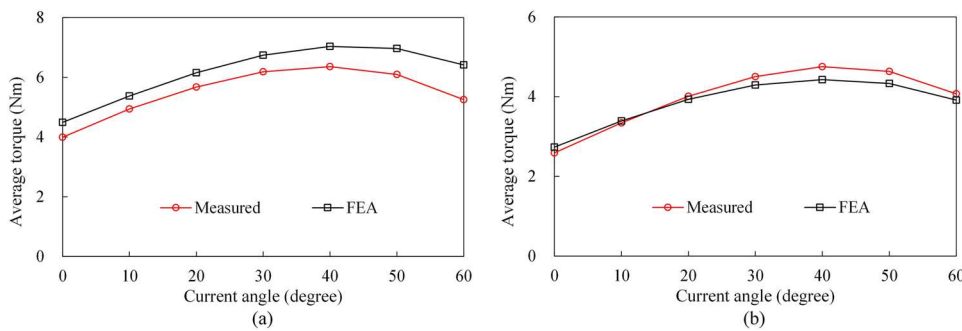


FIG. 11. Measured and FE-predicted average versus load current angle. (a) Flux-enhanced state. (b) Flux-weakened state.

maximum torque current angle is about 40 degree, which is identical with the FE results.

V. CONCLUSION

In this paper, the FBE of LCF PM on series hybrid magnet VFMM is revealed, which leads to the degradation of the torque density and the PM utilization ratio, and the causes of this phenomenon are revealed and further investigated. Due to the fact that magnetic energy product of LCF PM is much lower than that of HCF PM, when the two kinds of PMs contact closely, the magnetic reluctance of LCF PM will cause the reduction of the air-gap flux density and the MMF of LCF PM cannot compensate for the weakening effect. A DL hybrid magnet VFMM is further presented to prevent the air-gap flux reduction caused by the FBE of LCF PM. It can be found that the leakage flux path and dual-layer PM design are mainly responsible for the change of the equivalent magnetic circuit, which weakens the cross-coupling effect between HCF and LCF PMs. Therefore, the DL hybrid magnet VFMM can effectively reduce the FBE, resulting in the improvement of the torque density as well as the flux variation range. Finally, the experiments have been carried out to confirm the theoretical analyses.

ACKNOWLEDGMENTS

This study was supported by National Natural Science Foundation of China (52037002 and 52077033), Jiangsu Provincial Key Research and Development Program (BE2021052), “Thousand Talents Plan” Project of Jiangxi Province (jsxq2020102088),

Fundamental Research Funds for Central Universities of the Central South University (2242017K41003), High-end Foreign Experts Recruitment Plan of China (G2022141003L), Jiangsu Qing Lan Project (1116002211), “SEU Zhishan scholars” Program of Southeast University (2242019R40042), GF Key Laboratory of Science and Technology Foundation Project (6142217210201) and “the Excellence Project Funds of Southeast University”.

AUTHOR DECLARATIONS

Conflict of Interest

The authors have no conflicts to disclose.

Author Contributions

Yunrui Huang: Writing – original draft (equal). **Hui Yang:** Writing – original draft (equal); Writing – review & editing (equal). **Hao Zheng:** Formal analysis (equal); Investigation (equal). **Heyun Lin:** Supervision (equal). **Z. Q. Zhu:** Conceptualization (equal).

DATA AVAILABILITY

The data that support the findings of this study are available from the corresponding author upon reasonable request.

REFERENCES

- Z. Q. Zhu and D. Howe, “Electrical machines and drives for electric hybrid and fuel cell vehicles,” *Proc. IEEE* **95**(4), 746–765 (2007).

- ²K. T. Chau, C. C. Chan, and C. Liu, "Overview of permanent-magnet brushless drives for electric and hybrid electric vehicles," *IEEE Trans. Ind. Electron.* **55**(6), 2246–2257 (2008).
- ³M. Ehsani, K. M. Rahman, and H. A. Toliyat, "Propulsion system design of electric and hybrid vehicles," *IEEE Trans. Ind. Electron.* **44**(1), 19–27 (1997).
- ⁴W. L. Soong and N. Ertugrul, "Field-weakening performance of interior permanent-magnet motors," *IEEE Trans. Ind. Appl.* **38**(5), 1251–1258 (2002).
- ⁵T. M. Jahns, G. B. Kliman, and T. W. Neumann, "Interior permanent-magnet synchronous motors for adjustable-speed drives," *IEEE Trans. Ind. Appl.* **IA-22**(4), 738–747 (1986).
- ⁶V. Ostovic, "Memory motors," *IEEE Ind. Appl. Mag.* **9**(1), 52–61 (2003).
- ⁷N. Limsuwan, T. Kato, K. Akatsu, and R. D. Lorenz, "Design and evaluation of a variable-flux flux-intensifying interior permanent-magnet machine," *IEEE Trans. Ind. Appl.* **50**(2), 1015–1024 (2014).
- ⁸K. Sakai, K. Yuki, Y. Hashiba, N. Takahashi, and K. Yasui, "Principle of the variable-magnetic-force memory motor," in *2009 Proceedings of the International Conference on Electrical Machines and Systems (ICEMS)* (2009), pp. 1–6.
- ⁹A. Athavale, K. Sasaki, B. S. Gagas, T. Kato, and R. D. Lorenz, "Variable flux permanent magnet synchronous machine (VF-PMSM) design methodologies to meet electric vehicle traction requirements with reduced losses," *IEEE Trans. Ind. Appl.* **53**(5), 4318–4326 (2017).
- ¹⁰M. Ibrahim, L. Masisi, and P. Pillay, "Design of variable flux permanent magnet machine for reduced inverter rating," *IEEE Trans. Ind. Appl.* **51**(5), 3666–3674 (2015).
- ¹¹H. Hua, Z. Q. Zhu, A. Pride, R. Deodhar, and T. Sasaki, "A novel variable flux memory machine with series hybrid magnets," in *2016 Proceedings of the IEEE Energy Conversion Congress and Exposition (ECCE)* (2016), pp. 1–8.
- ¹²H. Yang, S. Lyu, H. Lin, Z.-q. Zhu, H. Zheng, and T. Wang, "A novel hybrid-magnetic-circuit variable flux memory machine," *IEEE Trans. Ind. Electron.* **67**(7), 5258–5268 (2020).
- ¹³H. Xu, J. Li, J. Chen, Y. Lu, and M. Ge, "Analysis of a hybrid permanent magnet variable-flux machine for electric vehicle tractions considering magnetizing and demagnetizing current," *IEEE Trans. Ind. Appl.* **57**(6), 5983–5992 (2021).
- ¹⁴H. Yang, H. Zheng, H. Lin, Z. Q. Zhu, and S. Lyu, "A novel variable flux dual-layer hybrid magnet memory machine with bypass airspace barriers," in *2019 Proceedings of the IEEE International Electric Machines and Drives Conference (IEMDC)* (2019), pp. 2259–2264.